Chapter 7
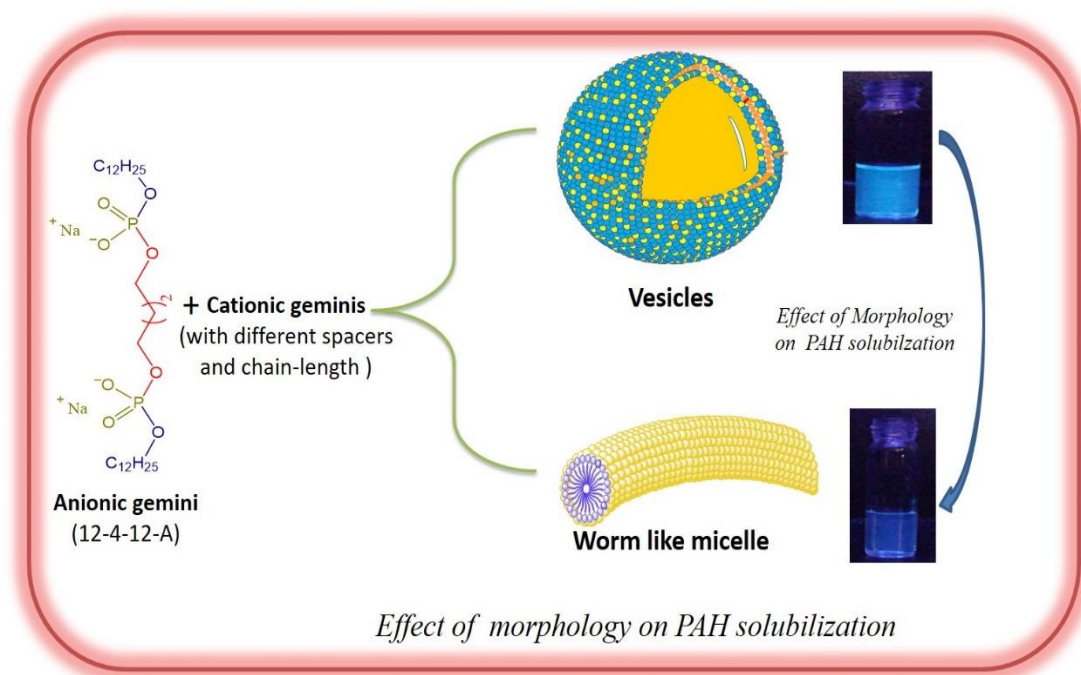
Solubilization of Polyaromatic Hydrocarbons in Various Morphologies Based on Mixed Gemini Surfactants

7.1. Introduction

Water/soil pollution by organic compounds (Polyaromatic hydrocarbons, dyes, and pesticides, *etc*), many of which are known to be toxic or carcinogenic, has caused considerable and worldwide concern. Contaminated water poses a serious threat to human health. Polycyclic aromatic hydrocarbons (PAHs) are ubiquitous environmental pollutants generated primarily during the incomplete combustion of organic materials (e.g. coal, oil, petrol, and wood) [1-3]. Among various methods, bioremediation is showing particular promise as a safe and cost-effective option. In spite of their xenobiotic properties, a variety of genera of gram-positive and negative bacteria, fungi and algae have been isolated and characterized for their ability to degrade PAHs. The general characteristics of PAHs are high melting point and boiling points (therefore they are solid), low vapor pressure, and very low *aqueous solubility* [4]. The aqueous solubility of PAHs decreases for each additional ring [5]. In order for bacteria to degrade any given PAH, it must be made available for uptake by the bacteria [6-8]. PAHs become bioavailable when they are in either the dissolved or the vapor phase. Photolysis reactions involving PAHs are similar to biodegradation reaction (i.e. the PAHs degrade more effectively when they are in the vapor or aqueous phase) [9]. The aqueous solubility and biodegradability of PAHs can be enhanced using surfactants, which comes under surfactant-enhanced remediation (SER). Surfactant micelles have a hydrophobic core, which helps to accumulate PAHs and increase the aqueous solubility. Therefore, SER is becoming a promising technique in removing PAHs from various media (e.g. soil and aqueous) and numerous studies have been conducted.

With the ever-increasing demand for chemical technologies, a renewed interest for better performing amphiphilic systems is growing. Solubilization of hydrophobic material into micellar aggregates has been studied for industrial, medicinal and

environmental applications. The solubilization efficacy decides the optimality of the surfactant system to make, insoluble organic material, bioavailable. Mixed surfactant systems have been proved superior from the solubilization point of view over individual components of the mixture [10-12]. Aqueous mixed surfactant systems have also been known to decontaminate the PAH polluted sites.

Recently, studies related to solubilization of PAHs are reported in aqueous cationic gemini mixtures [13, 14]. However, solubilization efficacy of oppositely charged gemini mixtures has not been exploited much [11, 15]. In one of these studies, it has been reported that mixing composition affects the micellar morphology with a concomitant influence on solubilization efficacy [15]. To the best of our knowledge, no attempt has been made to correlate the nature of the gemini spacer/ chain-length, resulting morphology (spherical-, ellipsoidal-, rod- or vesicles) and PAH solubilization efficacy in order to develop a morphology-solubilization efficacy relationship. Further, mixed vesicles are, probably, not utilized for the solubilization behavior of PAHs. No report has been found on co-solubilization of PAHs in vesicles and effect on size/shape of the aggregates post solubilization.
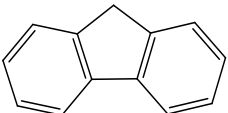
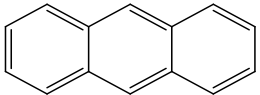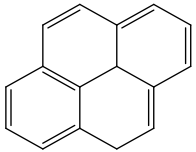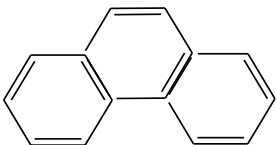The study constitutes a correlation of structure of mixed assemblies with an aqueous solubility of a typical PAH. For the purpose, various mixed gemini surfactant combinations are tried to enhance solubilization of different PAHs: anthracene; pyrene; fluorene and phenanthrene. A few co-solubilization experiments are also performed to study the influence on aqueous solubility in their mutual presence.

7.2. Results and Discussion

7.2.1. Solubilization in Single Aqueous Gemini Surfactant

Aqueous solubility, molar absorptivity coefficient (ε), partition coefficient (*n*-octanol-water system) and molecular structure of various PAHs are compiled in Table 1. Based on the compiled data hydrophobic character of PAHs will follow the order: Anthracene > Pyrene > phenanthrene > Fluorene. The aqueous solubility of PAH is expected to enhance in aqueous micellar solution which is interpreted in terms of the polarity of various micellar

Table 1. Structural formula and properties (molar extinction coefficient, ε) of polycyclic aromatic hydrocarbons (PAHs).

PAHs	Chemical structure and formula	M.W.[a] gm/mol	ε M^{-1}	Solubility mol/L	Log K_{ow}[c]
Fluorene	$C_{13}H_{10}$	166.22	2.15 x 10^4 at 262 nm	1.98 × 10^{-5}	4.18
Anthracene	$C_{14}H_{10}$	178.23	1.82 x 10^5 at 254 nm	2.53 × 10^{-7}	4.45
Pyrene	$C_{16}H_{12}$	204.27	4.71 x 10^4 at 264 nm	6.57 × 10^{-7}	5.18
Phenanthrene	$C_{14}H_{10}$	178.23	4.138 x 10^4	6.6 × 10^{-6}	4.46

[a]Molecular weight
[b]Aqueous solubility at 298 K
[c]Octanol-water partition co-efficient

interior regions. Micellar solubility is represented in the form of *molar solubilization ratio* (MSR) which is determined by the method given in **Chapter 2 (section 2.5.11, eq. 8).**

Typical absorbance (A) *vs* wavelength (λ) plots, for solubilized anthracene in different gemini surfactants (at fixed [gemini] = 10 mM), are shown in Figure 1(similar plots were obtained for other PAHs). MSR data of different PAHs in various individual Gemini surfactant are given in Table 2. All aqueous geminis show improved solubilization (than pure water) for each PAH which further depends on spacer nature, chain-length and morphology present. One single reason for enhanced solubilization of PAHs is the hydrophobic environment provided by micellar interior where hydrophobic PAH molecule can go and sit. Among all PAHs, fluorene shows higher MSR than others.
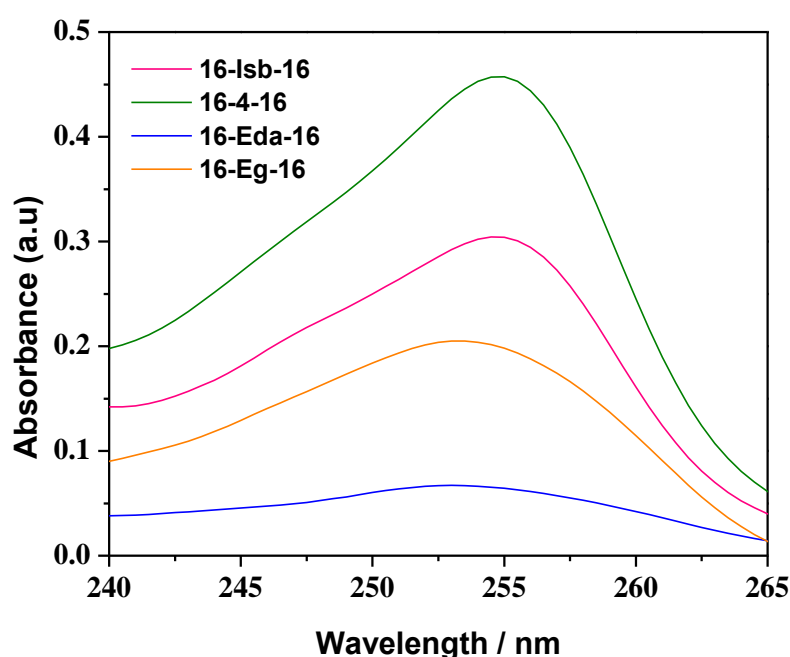

Figure 1. Representative UV-Visible spectra of PAH solubilized in 10 mM aqueous mixed gemini surfactant system

Table 2. Solubilization parameters (molar solubilization ratio, MSR; micelle-aqueous phase partition coefficient, ln K_m; Gibbs free energy, $\Delta G^o{}_s$) of 10 mM gemini surfactants in aqueous solution at 303 K.

Sr. No.	Gemini	Anthracene			Pyrene		
		MSR	ln K_m	-ΔG_s $\overline{\text{KJmol}^{-1}}$	MSR	ln K_m	-ΔG_s $\overline{\text{KJmol}^{-1}}$
1	12-4-12A	0.026	8.86	22.33	0.038	10.15	25.58
2	12-4-12	0.009	12.76	31.63	0.0443	12.69	31.44
3	16-4-16	0.026	8.84	22.29	0.109	27.22	68.60
4	16-Isb-16	0.014	8.21	20.69	0.075	19.45	49.02
5	16-Eg-16	0.003	6.77	17.05	0.016	8.39	21.14
6	16-Eda-16	0.009	7.76	19.56	0.057	9.64	24.29

Aggregate–bulk water partition coefficient (K_m) denotes the solubilization by the micellar phase. K_m represent the ratio of mole fractions of the PAH in the micelle (X_m) and bulk aqueous phases (X_a). X_m can be correlated with MSR as X_m = MSR/ (1 + MSR). X_a can be computed by its relation with S_{cmc} and V_m (X_a = [S_{cmc}] V_m, where V_m is the molar volume of water (0.01807 L mol^{-1}) at 30 °C). Therefore, K_m can be written as [16]

$$K_m = \text{MSR}/\{[S_{cmc}]V_m\,(1 + \text{MSR})\} \tag{1}$$

K_m can be used to determine standard free energy change of the solubilisation process (ΔG_s^0) by using follthe owing exprthe ession

$$\Delta G_s^o = -RT \ln K_m \tag{2}$$

The values of K_m and ΔG_s^0 are also complied in Tables 2. The negative value of ΔG_s^0, with each individual gemini, shows that the phenomenon of PAH solubilisation is spontaneous in nature.

7.2.2. Solubilization in Oppositely Charged Mixed Aqueous Geminis

Typical plots of A *vs* λ for different PAHs solubilization in oppositely charged mixed aqueous geminis (16-Eda-16 + 12-4-12A) at different mole fractions (X = 0-1) are shown in Figure 2(a-d) Similar plots were obtained with other gemini mixtures (having cationic gemini with 16 carbon atom) with different PAHs. Even on decreasing the chain length of the cationic component of the mixture (12-4-12 +12-4-12A), the trend does not change much (Figure 3a& b). Comparing the absorbance data for single gemini and binary mixtures, it can be seen that higher absorbance is found with aqueous mixed geminis. However, absorbance changes are random and not directly related to composition. This is due to the presence of different morphologies in the solution as discussed in **Chapter 6.**
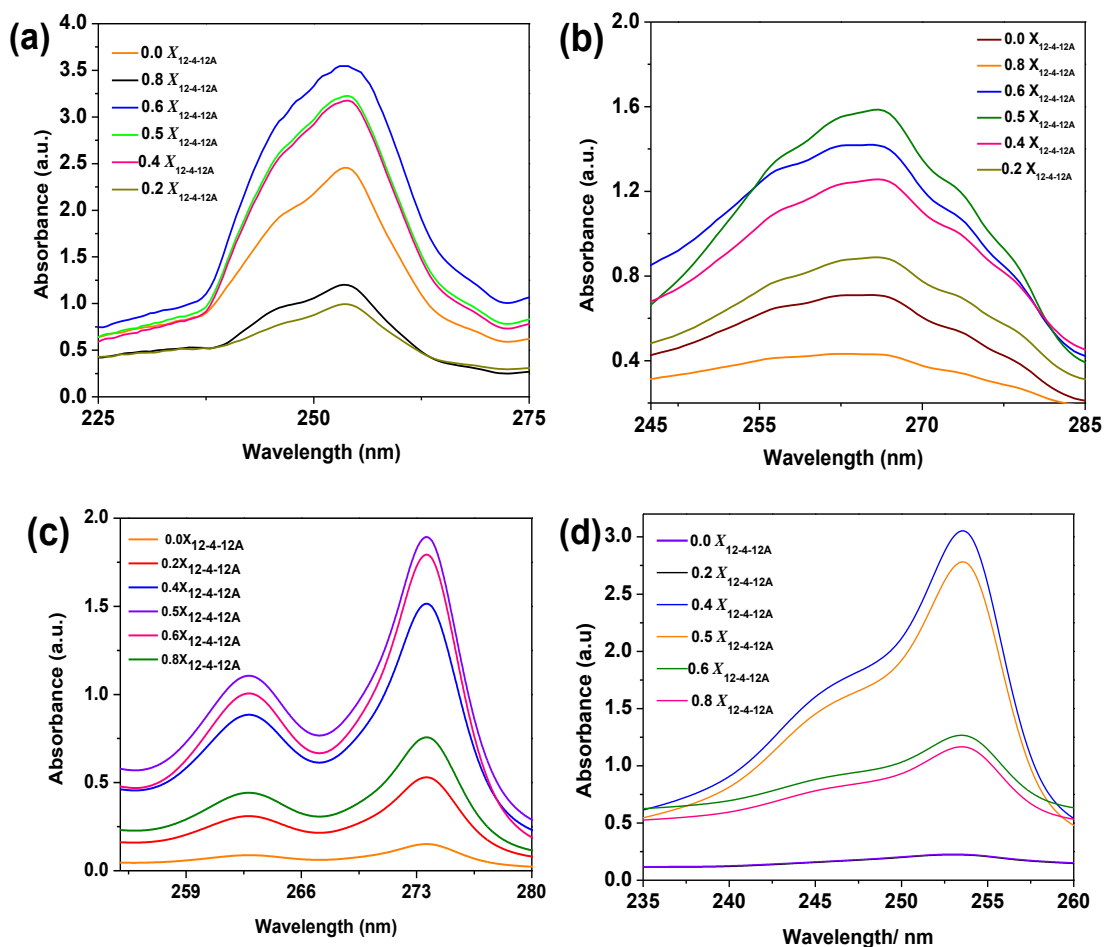
Figure 2. Representative UV-Visible spectra of PAH solubilized in 10 mM aqueous mixed gemini surfactant system at different mole fractions of anionic gemini ($x_{12\text{-}4\text{-}12A}$) with cationic gemini surfactants 16-Eda-16, a) Phenanthrene, (b) Fluorene (c) pyrene, and (d) anthracene.

Table 3. Solubilization parameters (molar solubilization ratio, MSR; micelle-aqueous phase partition coefficient, ln K_m; Gibbs free energy, ΔG^o_s) of 10 mM single and mixed gemini surfactants in aqueous solution at 303 K.

$x_{12\text{-}4\text{-}12\text{-}A}$	Morphology	Anthracene			Pyrene			Fluorene			Phenanthrene		
		MSR	ln K_m	$-\Delta G_s$ KJmol^{-1}	MSR	ln K_m	$-\Delta G_s$ KJmol^{-1}	MSR	ln K_m	$--\Delta G_s$ KJmol^{-1}	MSR	lnK_m	$--\Delta G_s$ KJmol^{-1}
							16-4-16						
1.0	Ellipsoidal	0.026	8.86	22.33	0.038	10.15	25.58	0.091	10.36	26.09	0.049	9.49	23.92
0.8	Rod	0.028	8.94	22.52	0.058	15.07	37.98	0.071	9.82	24.74	0.152	10.63	26.78
0.6	Rod	0.028	8.91	22.46	0.086	21.84	55.05	0.108	10.20	25.71	0.223	11.05	27.85
0.4	Vesicle	**0.032**	9.06	22.83	**0.171**	40.32	101.62	**0.254**	10.94	27.56	**0.233**	11.01	27.74
0.2	Rod	0.026	8.84	22.29	0.143	34.53	87.03	0.149	10.49	26.42	0.081	9.99	25.19
0.0	Rod	0.026	8.84	22.29	0.109	27.22	68.60	0.159	10.54	26.57	0.190	10.84	27.33
							16-Isb-16						
0.8	Ellipsoidal	0.013	8.18	20.62	0.064	16.64	41.94	0.189	10.69	26.91	0.045	9.39	23.67
0.6	Rod	**0.028**	8.91	22.46	0.065	16.96	42.75	**0.195**	10.72	27.01	**0.142**	10.55	26.59
0.4	Rod	0.026	8.86	22.32	**0.084**	21.44	54.04	0.168	10.59	26.69	0.096	10.16	25.60
0.2	Ellipsoidal	0.027	8.87	22.37	0.060	15.56	39.22	0.113	10.24	25.80	0.072	9.87	24.88
0.0	Ellipsoidal	0.014	8.21	20.69	0.075	19.45	49.02	0.128	10.35	26.09	0.079	9.97	25.11

Table.4 Solubilization parameters (molar solubilization ratio, MSR; micelle-aqueous phase partition coefficient, ln K_m; Gibbs free energy, ΔG^o_s) of 10 mM single and mixed gemini surfactants in aqueous solution at 303 K

| $x_{12\text{-}4\text{-}12\text{-}A}$	Morphology	Anthracene			Pyrene			Fluorene			Phenanthrene		
		MSR	ln K_m	$-\Delta G_s$ KJmol^{-1}	MSR	ln K_m	$-\Delta G_s$ KJmol^{-1}	MSR	ln K_m	$--\Delta G_s$ KJmol^{-1}	MSR	lnK_m	$--\Delta G_s$ KJmol^{-1}
							16-Eda-16						
1.0	Ellipsoidal	0.026	8.85	22.32	0.038	9.24	23.28	0.091	10.11	25.48	0.049	9.49	23.92
0.8	Ellipsoidal	0.012	7.94	20.00	0.041	9.31	23.47	0.131	10.38	26.16	0.076	9.88	24.90
0.6	Vesicle	**0.022**	8.69	21.89	0.096	10.16	25.61	0.180	10.65	26.84	0.236	10.88	27.42
0.5	Vesicle	**0.031**	9.03	22.76	**0.170**	10.37	27.05	**0.316**	11.36	28.61	**0.334**	11.41	28.75
0.4	Vesicle	0.016	8.36	21.07	0.102	10.22	25.76	**0.200**	10.74	27.06	0.261	10.95	27.59
0.2	Ellipsoidal	0.011	8.03	22.24	0.062	9.73	24.51	0.060	9.66	24.35	0.088	10.01	25.22
0.0	Ellipsoidal	0.009	7.76	19.56	0.057	9.64	24.29	0.099	10.13	25.53	0.179	10.65	26.84
							16-Eg-16						
0.8	Ellipsoidal	0.0012	5.76	14,53	0.011	7.97	20.08	0.106	10.1	25.55	0.260	10.96	27.62
0.6	Ellipsoidal	**0.0154**	8.35	21.03	0.008	7.68	19.35	**0.089**	10.0	25.27	0.125	10.34	26.06
0.4	Ellipsoidal	0.0051	7.25	18.27	**0.032**	9.07	22.86	0.121	10.3	25.98	0.109	10.21	25.73
0.2	Ellipsoidal	0.0038	6.97	17.56	0.0067	7.44	18.75	0.050	9.49	23.90	0.114	10.26	25.85
0.0	Ellipsoidal	0.0032	6.77	17.05	0.016	8.39	21.14	0.101	10.15	25.57	0.176	10.63	26.79
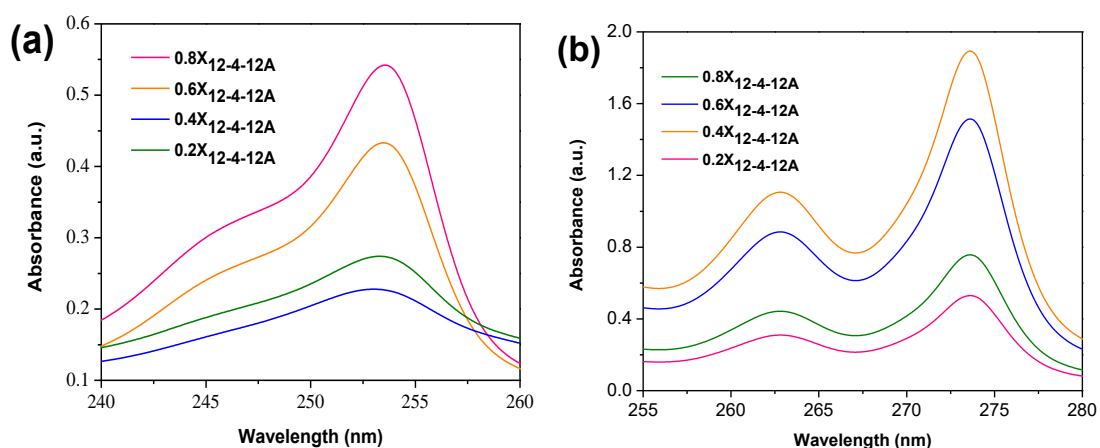
Figure 3. UV-Visible spectra of solubilized (a) anthracene (b) pyrene, in 10 mM aqueous mixed gemini surfactant system (12-4-12 + 12-4-12A) at different mole fractions of anionic gemini ($x_{12\text{-}4\text{-}12A}$).

Table.5 Solubilization parameters (molar solubilization ratio, MSR, micelle-aqueous phase partition coefficient, ln K_m; Gibbs free energy, $\Delta G^o_{s)}$ of 12-4-12 in single or mixed form.

$x_{12\text{-}4\text{-}12\text{-}A}$	Morphology	Anthracene			Pyrene		
		MSR	ln K_m	$-\Delta G_s$ KJmol^{-1}	MSR	ln K_m	$-\Delta G_s$ KJmol^{-1}
0.0	Spherical	0.0088	12.76	31.63	0.0443	12.69	31.44
0.2	Ellipsoidal	0.0054	13.98	35.21	0.0894	15.75	39.67
0.4	Vesicles	**0.0849**	16.67	41.96	0.0499	15.20	38.30
0.6	Vesicles	0.0226	15.39	38.77	0.1389	16.15	40.67
0.8	Ellipsoidal	0.0536	16.23	40.88	0.0237	14.48	36.48

MSR data with binary gemini mixtures Tables 3-5. MSR data show higher values with oppositely charged mixed gemini systems over individual components of the mixture (Table 2). This is in consonance with the earlier report with similar gemini mixtures [11]. However, differences in MSR values may be due to the fact that the

earlier study has been conducted at just above the CMC where, predominantly, spherical micelles would have been present. Different concentration range, as well as a change in the morphology (rod-shaped or vesicles), are responsible for the differences in the MSR data. Larger aggregates (in the present study), with higher hydrophobic volume than the individual gemini surfactant micelles, are responsible for the effective solubilization of PAH and higher MSR values (Tables 3-5). Among all gemini mixtures, vesicular systems have been found more effective than the one having other morphologies (ellipsoidal or rod). MSR follows the order: vesicles > rod-shaped- > ellipsoidal- > spherical micelles. This reveals a synergistic effect of mixing of two oppositely charged gemini surfactant (of optimum composition), with an appropriate spacer, resulting vesicular aggregates. Among different PAHs, MSR has been found to be dependent on the polarity and geometrical size of an individual PAH.

The aqueous solubility trend (Table 1), for various PAHs, was observed even with various mixed gemini surfactants (having 12-4-12A as one of the components. However, the maximum MSR (or solubility) has been found in most cases when the composition of the two components of the mixture was in the mole fraction range of 0.4 to 0.6 (Table 3-5). As discussed in the previous chapter (Chapter 6), vesicular aggregates or rod-shaped micelles are formed in this composition range. Therefore, composition/ morphology plays a decisive role in solubilizing the PAHs. However, it may be mentioned here that these aggregates are not formed with all the cationic gemini surfactants. Morphological data (SANS, DLS or TEM) clearly indicate that gemini with polymethylene and Eda spacers form vesicles at an appropriate composition of the mixture while the other two Isb and Eg formed ellipsoidal or rod-shaped micelles with a similar composition and chain-length. However, a mixture with equal chain-lengths (12-4-12A + 12-4-12) shows distinctly higher MSR for anthracene (Table. 5) at the

same mixture composition (0.6 $X_{12\text{-}4\text{-}12}$). This composition forms multilamellar vesicles (with inter-layer distance d= 37.4 Å) with higher size (D_H = 292 nm). Such aggregates have higher hydrophobic volume and responsible for higher anthracene solubility. However, pyrene fails to show this trend though its solubility was enhanced in comparison to the aqueous phase. Probably, the solubilization site has a role to play in micellar solubilization. Apart from the above factors (composition, morphology, alkyl chain-length (m), nature of PAHs and structure of the spacer), solubilization sites of each PAH have equal importance in overall solubilization phenomenon [17, 18]. It may be mentioned here that a typical surfactant(s) aggregate can be considered as made up of various layers of different polarities (highly polar- *head group region* to highly nonpolar- *micellar core*) [19-21]. This polarity variation can be affected by the hydrocarbon tail length, nature of the head group as well as the nature of the spacer. Probably, most of the factors are contributing to the PAH solubilization in the mixture of oppositely charged gemini surfactants as reported for other similar systems [22]. MSR data reported for typical PAH (anthracene or pyrene) have been compiled and compared with the present surfactant systems (Table 6) [10-12, 17, 23]. Present systems are undoubtedly better than the similar systems available in the literature. Moreover, one of the systems (having 16-Eda-16 + 12-4-12A) shown similar efficacy (towards vesicle formation as well as MSR) though it contains a biodegradable spacer (-Eda-) [10]. This indicates that less biodegradable spacer containing gemini can be replaced by the above system without losing the efficacy towards hydrophobic molecule solubilization. To get further insight regarding the site of solubilization, co solubilization (solubilization of one PAH in presence of the other) experiment has also been performed and the data are discussed.

Table 6. Comparative MSR data available from various studies for the solubilization of Anthracene and Pyrene in mixed oppositely charged surfactant systems in an aqueous medium.

System[a]	MSR		Ref.
	Anthracene	**Pyrene**	
16-Eda-16+SDS	0.0248	0.0576	[10]
16-Eda-16+SDBS	0.0243	0.0745	
16-4-16+AOT	0.016	0.047	[23]
16-5-16+AOT	0.0119	0.0323	
16-6-16+AOT	0.0103	0.0526	
12-Eda-12+SDS	0.0061	0.0137	[17]
12-Eda-12+SDBS	0.0049	0.0112	
16-4-16 (0.7) +12-4-12A (0.3)	0.0148	0.1023	[11]
16-Eda-16 (0.6) +12-4-12A (0.4)	0.0147	0.0813	
12-4-12 + SC	0.002	0.014	
14-4-14 + SC	0.004	0.021	
16-4-16 + SC	0.005	0.030	
12-Eda-12 + SC	0.002	0.011	
14-Eda-14 + SC	0.003	0.016	
16-Eda-16 + SC	0.004	0.023	[12]
12-4-12 + SDC	0.002	0.013	
14-4-14 + SDC	0.003	0.020	
16-4-16 + SDC	0.005	0.029	
12-Eda-12 + SDC	0.002	0.011	
14-Eda-14 + SDC	0.003	0.015	
16-Eda-16 + SDC	0.004	0.023	
16-4-16 (0.6) + 12-4-12A (0.4)	**0.0321**	**0.1706**	
16-Isb-16 (0.4) + 12-4-12A (0.6)	0.0276	0.085 (0.4 $x_{12\text{-}4\text{-}12A}$)	
16-Eda-16 + 12-4-12A	**0.031**	**0.170**	[present study]
12-4-12 (0.6) + 12-4-12A (0.4)	**0.085**	0.139 (0.6 $x_{12\text{-}4\text{-}12A}$)	

7.3. Co-solubilization of PAHs in the Mixed Gemini Surfactant System

Co-solubilization of a pair of PAHs (pyrene and anthracene) are performed in two gemini mixtures (one each from 16-polymethylene/ Eda-16 and 16-Isb/Eg-16). The co-solubilization data are compiled in Table 7. Data show that solubilization of an individual PAH can increase or decrease on co-solubilization of another PAHs. As mentioned earlier, the solubilization site of a particular PAH has a role to play in the co-solubilization of more than one PAH. If the solubilization site is common for the PAHs in the pair, the solubilization content of one of them may decrease. However, if the two PAHs has different micellar solubilization sites, their mutual presence may increase solubilization content due to increased hydrophobic interactions caused by the presence of PAHs. This indeed was observed in Table 7.

Table 7. MSR values of anthracene and pyrene individually and their mutual presence at various mole fractions of gemini mixtures.

$x_{12\text{-}4\text{-}12\text{-}A}$	**Morphology**	**MSR**			
		Anth	Anth-Pyr	Pyr	Pyr-Anth
16-Eda-16					
0.8	Ellipsoidal	0.010	0.013	0.041	0.062
0.6	Vesicles	0.022	0.026	0.096	0.058
0.5	Vesicles	**0.031**	**0.049**	**0.170**	**0.171**
0.4	Vesicles	0.016	0.023	0.102	0.044
0.2	Ellipsoidal	0.011	0.013	0.062	0.048
0.0	Ellipsoidal	0.009	0.011	0.057	0.035
16-Eg-16					
0.8	Ellipsoidal	0.0012	0.009	0.011	0.014
0.6	Ellipsoidal	**0.0154**	**0.018**	0.008	0.019
0.4	Ellipsoidal	0.0051	**0.015**	**0.032**	0.046
0.2	Ellipsoidal	0.0038	0.016	0.007	0.039
0.0	Ellipsoidal	0.0032	0.011	0.016	0.040

Here, MSR values of anthracene increase in the presence of pyrene. Additionally, pyrene solubilization (singly or with anthracene) shows increase or decrease depending upon system composition. However, the vesicular system shows a significant increase in MSR of anthracene in the presence of pyrene. Contrary to this, MSR of pyrene shows composition dependence in the presence of anthracene. A similar trend was observed with mixtures of equal chain-length geminis (Table 8).

Table 8: MSR data of co-solubilization of anthracene and pyrene in 10 mM gemini surfactant system at various mole fractions of $x_{12-4-12A}$.

| System	MSR	
$x_{12-4-12A}$	*Anthracene*	*Pyrene*
0.2	0.0114	0.0291
0.4	0.0367	0.0644
0.6	0.0395	0.0578
0.8	0.0446	0.0309

7.4. Vesicles Size Variation After PAH Solubilization

As mentioned above, vesicular systems show higher solubilization efficacy with each PAH. SANS data (Figure 4) are collected in order to get an idea about the vesicle thickness variation on solubilizing PAH. Data of Table.9 show that vesicles forming system have charges of the different signs (+ or -). The negative vesicles show nearly no change in bilayer thickness due to the solubilization of anthracene or pyrene. However, positively charged vesicles show significant changes in bilayer thickness with the solubilization of anthracene or pyrene. This may be due to electrostatic repulsion between electron cloud of PAH and head group charge of the mixed vesicles. In the former case (0.4 $X_{16-eda-16}$) this repulsion in the vesicular interior has less effect

on bilayer thickness as indeed observed. On the other side in case of positive vesicles, one can expect electrostatic attraction between the vesicular head and electron cloud of a typical PAH. This may predominant hydrophobic interaction and responsible for higher bilayer thickness. However, when one PAH is added in the presence of another bilayer thickness shows a significant reduction. More data are needed to generalize the trend. It may be mentioned here that electrostatic interaction (repulsion or attraction) may change the polarity of the vesicular aggregates and hence interaction and solubilization site of the PAH. Therefore, aggregate (vesicles or micelle) electrostatics is needed before optimizing the solubilization process for a typical hydrophobic solubilizate. A combined effect of all the above factors seems responsible for the trend shown by the data of Table 8. A possible site for solubilization of PAHs in vesicles is shown in scheme 1.

Table 9. PAH(s) solubilization effect on Bi-layer thickness of vesicles in aqueous solution at 303K.

System	Zeta-potential	Bi-layer thickness (Å)				
		Without PAH	Anth	Pyr	Anth-Pyr	Pyr-Anth
0.4 $x_{16\text{-Eda-}16}$	-44.8	22.0	21.7	22	22.3	21.8
0.6 $x_{16\text{-Eda-}16}$	+57.3	23.0	19.7	62.5	22.5	21.2
0.6 $x_{16\text{-}4\text{-}16}$	+79.4	25.0	55.4	38.7	-	-
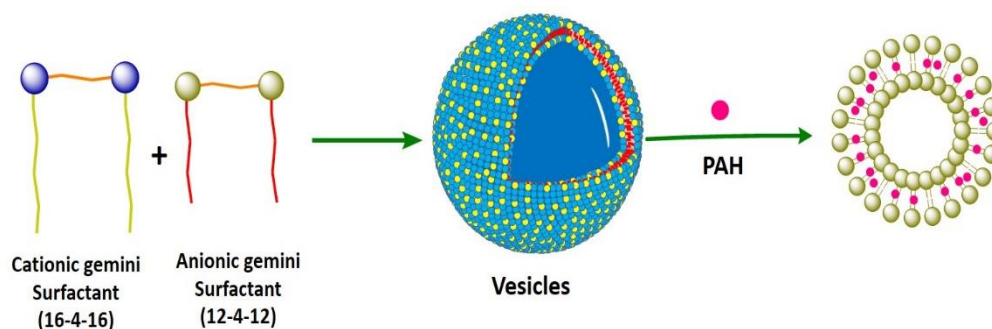
Scheme 1. Schematic Representative PAH Solubilization Site in Vesicle Bilayer
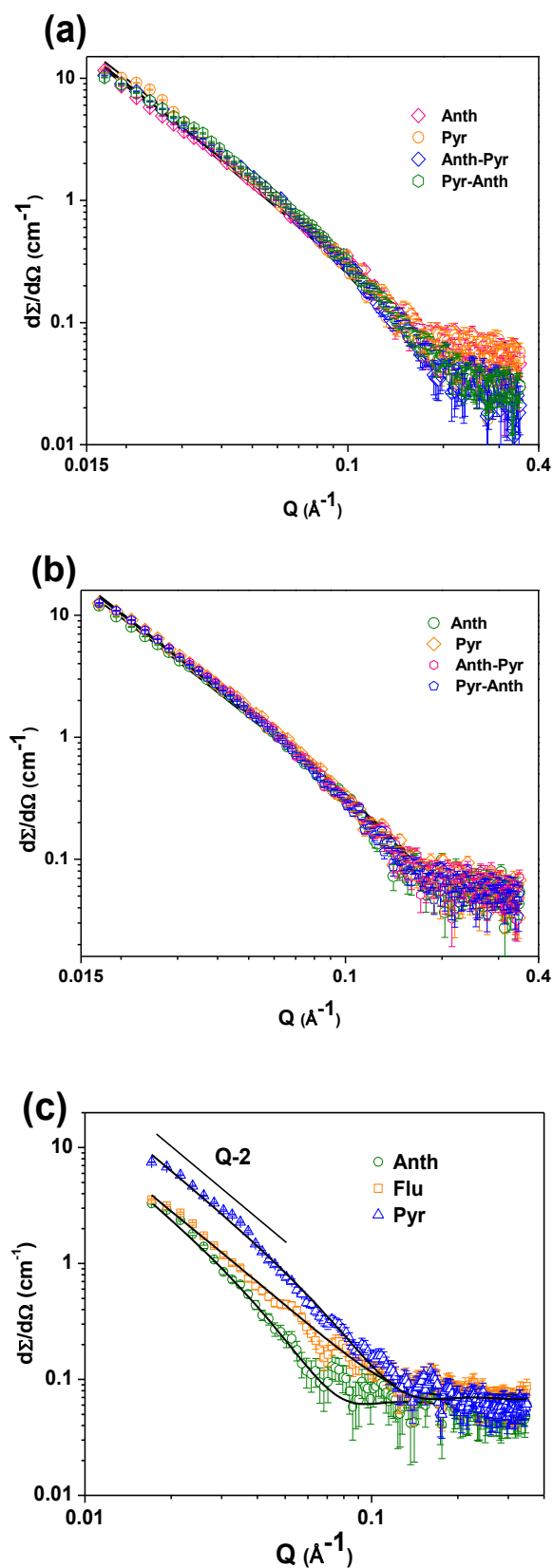
(a)

(b)

(c)

Figure 4. SANS spectra of 10 mM aqueous mixed gemini surfactant system (16-Eda-16 + 12-4-12A) after solubilizing PAHs **(a)** 0.4 x $_{16\text{-Eda-16}}$ **(b)** 0.6 x $_{16\text{-Eda-16}}$ (c) 0.6 x 16-4-16.

7.5. Conclusion

Based on the studies compiled in Chapter 6, various gemini compositions with typical morphologies are used to study the solubilization behavior of different PAHs in an individual and mixed state. All PAHs show enhanced aqueous solubility in micellar or mixed micellar systems (solubility follow the order: water < micellar solution < mixed micellar solution). Analysis of MSR data clarifies that mixed systems, with vesicle morphology, solubilized PAH preferentially over rod-shaped or ellipsoidal (spherical) micelle. Since morphologies are dependent on spacer nature (or chain length of the alkyl tail), the magnitude of solubility enhancement (**Scheme. 2**) can directly be correlated with molecular architecture of cationic gemini surfactant (as another component, 12-4-12A, is common for all the combinations). Among PAHs, solubilization efficacy of the surfactant systems is dependent on the polarity and site of solubilization (of the PAH). MSR (of co-solubilized PAHs) also gives an idea about the variation of solubility of a PAH in the presence of another one. The strategies adopted here can be extended towards the solubilization of other hydrophobic materials such as dyes, drugs or pesticides.
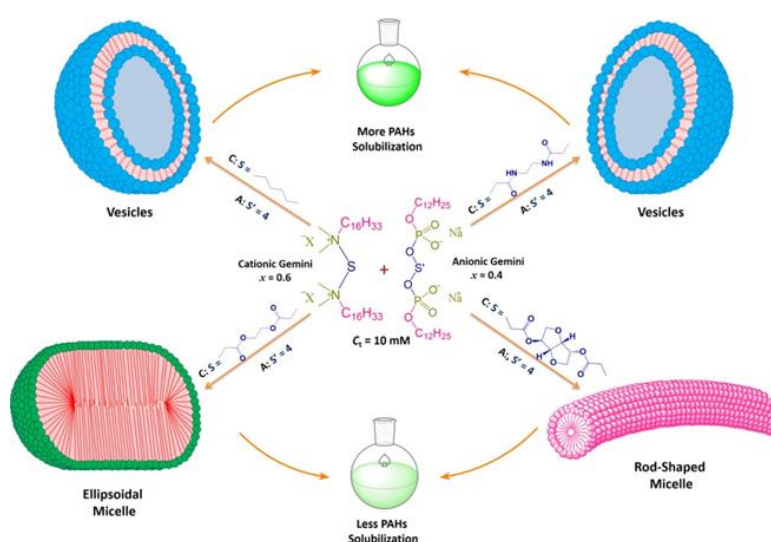
Scheme 2. Morphology-dependent PAH solubilization.

References

[1] A. Baklanov, O. Hänninen, L. Slørdal, J. Kukkonen, N. Bjergene, B. Fay, S. Finardi, S. Hoe, M. Jantunen, A. Karppinen, *Atmospheric Chem. Phys.* 2007, 7, 855-874.

[2] J.S. Latimer, J. Zheng, and Fate of PAHs in the Marine Environment, *PAHs: an ecotoxicological perspective,* 2003, 9.

[3] C.A. Menzie, B.B. Potocki, J. Santodonato, *Environ. Sci. Technol.* 1992, 26, 1278-1284.

[4] J. Masih, R. Singhvi, K. Kumar, V. Jain, A. Taneja, *Aerosol Air Qual Res.* 12 (2012) 515-525.

[5] J. Masih, A. Masih, A. Kulshrestha, R. Singhvi, A. Taneja, *J. Hazard. Mater.* 2010, 177,190-198.

[6] C. Cerniglia, The utilization of bioremediation to reduce soil contamination: Problems and solutions, *Springer*,2003, 51-73.

[7] C.E. Dandie, S. Thomas, R. Bentham, N. McClure, *J. applied microbiology,* 2004, 97,246-255.

[8] L. Fredslund, K. Sniegowski, L.Y. Wick, C.S. Jacobsen, R. De Mot, D. Springael. *Microbiol.Res*, 2008, 159, 255-262.

[9] B.J. Finlayson-Pitts, J.N. Pitts. *Science*, 1997, 276, 1045-1051.

[10] W.H. Ansari, N. Fatma, M. Panda. *Soft Matter* 2013, 9, 1478-1487.

[11] S.K. Yadav, K. Parikh, S. Kumar, *Colloid. Surf. A.* 2017, 514, 47-55.

[12] S.K. Yadav, K. Parikh, S. Kumar, *Colloid. Surf. A.* 2017, 522,105-112.

[13] M. Panda, N. Fatma, *J. Mol. Struct.* 2016, 1115, 109-116.

[14] J. Wei, G. Huang, C. An, H. Yu. *J. Hazard. Mater.*2011, 190, 840-847.

[15] S. Singh, A. Bhadoria, K. Parikh, S.K. Yadav, S. Kumar, V.K. Aswal, S. Kumar, *J. Phy.Chem. B* 2017, 121, 8756-8766.

[16] D. A. Edwards, R.G. Luthy, Z. Liu. *Environ. Sci. Technol*. 1991, 25, 127-133.

[17] N. Fatma, M. Panda, W.H. Ansari. *Colloid. Surf. A.* 2015, 467, 9-17.

[18]R. Masrat, M. Maswal, A.A. Dar. *J. Hazard. Mater.* 2013, 244, 662-670.

[19] R. Nagarajan. *Curr. Opin. Colloid Interface Sci.* 1997, 2, 282-293.

[20] C.V. Teixeira, R. Itri, L.Q. do Amaral. *Langmuir* 2000, 16, 6102-6109.

[21] G. Cerichelli, G. Mancini. *Langmuir* 2000, 16,182-187.

[22] X. Liang, C. Guo, S. Liu, Z. Dang, Y. Wei, X. Yi, S. Abel. *J. Mol. Liq.* 2018, 263,1-9.

[23] M. Panda. *J. Mol. Liq.* 2013, 187, 106-113.